Aerotaxy - A Gas-Phase Nanowire Growth Technique

Heurlin, Magnus

2014

Aerotaxy

A Gas-Phase Nanowire Growth Technique

LUND
UNIVERSITY

by

Magnus Heurlin

Licentiate thesis

Division of Solid State Physics
Department of Physics
Lund University
Sweden 2014

Abstract

In this thesis an efficient nanowire fabrication technique, called Aerotaxy, is investigated. Traditional nanowire fabrication techniques include the use of a substrate as a point of nanowire nucleation which limits the amount of nanowires that can be produced per unit time. In contrary, Aerotaxy offers a continuous growth process, in the gas-phase, which could substantially increase the rate at which nanowires are fabricated and thus lower their fabrication cost.

Investigations of nanowire properties such as size, shape and crystal structure, with electron microscopy, show that growth can be controlled and tuned to a high degree. Optical properties investigated with photoluminescence reveal that as-grown nanowires have good optical properties and excellent spectral uniformity. Aerotaxy can thus be used to produce high-quality nanowires, that could be integrated into future opto-electronic devices, at a lower cost than other growth techniques offer.

Contents

List of papers

This thesis is based on the following article.

I. Continuous gas-phase synthesis of nanowires with tunable properties

Magnus Heurlin, Martin H. Magnusson, David Lindgren, Martin Ek, L. Reine Wallenberg, Knut Deppert and Lars Samuelson

Nature 492, 90–94 (2012)

I participated in planning and coordination of the project, performed most of the nanowire growth and electron microscopy investigations. I wrote the main part of the paper.

The following articles are not included since they deal with topics beyond the scope of this thesis. They are listed in chronological order.

II. Axial InP nanowire tandem junction grown on a silicon substrate

Magnus Heurlin, Peter Wickert, Stefan Fält, Magnus T. Borgström, Knut Deppert, Lars Samuelson, and Martin H. Magnusson

Nano Letters 11, 2028–2031 (2011)

III. Nanowires with promise for photovoltaics

Magnus T. Borgström, Jesper Wallentin, **Magnus Heurlin**, Stefan Fält, Peter Wickert, Jack Leene, Martin H. Magnusson, Knut Deppert, and Lars Samuelson

IEEE Journal of Selected Topics in Quantum Electronics 17, 1050-1061 (2011)

IV. InAs quantum dots and quantum wells grown on stacking-fault controlled InP nanowires with wurtzite crystal structure

Kenichi Kawaguchi, **Magnus Heurlin**, David Lindgren, Magnus T. Borgström, Martin Ek, and Lars Samuelson

Applied Physics Letters 99, 131915 (2011)

V. Growth of InAs/InP core–shell nanowires with various pure crystal structures

Sepideh Gorji Ghalamestani, **Magnus Heurlin**, Lars-Erik Wernersson, Sebastian Lehmann, and Kimberly A Dick

Nanotechnology 23, 285601 (2012)

VI. Spatially resolved Hall effect measurement in a single semiconductor nanowire

Kristian Storm, Filip Halvardsson, **Magnus Heurlin**, David Lindgren, Anders Gustafsson, Phillip M. Wu, Bo Monemar, and Lars Samuelson

Nature Nanotechnology 7, 718-722 (2012)

VII. Reflection measurements to reveal the absorption in nanowire arrays

Nicklas Anttu, Azhar Iqbal, **Magnus Heurlin**, Lars Samuelson, Magnus T. Borgström, Mats-Erik Pistol, and Arkady Yartsev

Optics Letters 38, 1449-1451 (2013)

VIII. Optical far-field method with subwavelength accuracy for the determination of nanostructure dimensions in large-area samples

Nicklas Anttu***, Magnus Heurlin***, Magnus T. Borgström, Mats-Erik Pistol, H. Q. Xu, and Lars Samuelson

Nano Letters 13, 2662-2667 (2013)

*These authors contributed equally.

IX. Optical characterization of InAs quantum wells and dots grown radially on wurtzite InP nanowires

David Lindgren, Kenichi Kawaguchi, **Magnus Heurlin**, Magnus T Borgström, Mats-Erik Pistol, Lars Samuelson, and Anders Gustafsson

Nanotechnology 24, 225203 (2013)

Acknowledgments

This is perhaps the most difficult part to write. However, since there are more things to come in the next few years I will try to keep it short.

I would like to start by thanking my main supervisor Lars Samuelson for being an unlimited source of new and sometimes a bit "crazy" ideas. It is when you have an idea no one else believes will work, that you have a unique opportunity to advance science and technology in a leap instead of baby steps.

Magnus Borgström and Martin Magnusson have been my steady points during day to day operations during the past years. Your valuable insights about small and big things in science and everyday life helps to propel me forward.

Knut Deppert is acknowledged for his vast knowledge about aerosols and for always being so generous and friendly. Without you the aerotaxy project would not have been so successful.

Reine Wallenberg, Martin Ek and Gunnel Karlsson at the Division of Polymer & Materials Chemistry has contributed to analysis on the atomic scale of our tiny nanowires. With you there is no need to squint ones eyes to see the atoms.

At FTF I would especially like to thank David for our numerous collaborations as well as my fellow growers Sebastian, Kenichi, Daniel, Jesper, Alexander and Sepideh. In addition Nicklas, Kristian, Olof, Ali, Vishal, Bahram, Ofogh, Reza and the "Minority Carriers" have all contributed, both in science and for creating a nice work environment.

Finally a few words about the most important people in the world, Camilla, Tage and Ebbe. I love you all!

1 Introduction

1.1 Nanotechnology

Nanotechnology is a field of science where the major disciplines chemistry, biology and physics have converged. By using knowledge and techniques from these traditionally different parts of science entirely new phenomena can be discovered, studied, understood and finally utilized to improve everyday life. This thesis is written in the borderland between physics and chemistry and methods developed in both these fields are required to fabricate and study the nanostructures, also known as nanowires, described in the following chapters.

Semiconductor nanowires present a new way of forming different materials commonly used for electronic, photovoltaic and light emitting devices. Besides new ways of forming the material, nanowires also offer new possibilities in controlling and tuning their physical and chemical properties. Nanowires studied in this thesis are typically crystalline and have a diameter below 100 nm and length around 1 µm. This places them in a regime where small changes in size or shape can have a large influence on the material properties.

The focus of this thesis is on an efficient fabrication method of these small nanostructures. Besides fabricating them in an efficient way it is also shown that their size, shape and crystal structure can be controlled while also achieving good material properties.

1.2 Crystal Growth

Crystal growth is governed by thermodynamics and a systems´ strive to reach equilibrium. In crystal growth at least two phases are present, a supply phase and a crystal phase. A system is at equilibrium when its Gibbs free energy (G) is at a minimum. The small change in G that occurs when material (N) is added to a system is described by the chemical potential (μ) defined as:

$$\mu = \frac{\partial G}{\partial N}_{T,p} \tag{1.1}$$

The subscript T,p denotes that the temperature and pressure in the system are kept constant. The difference in chemical potential between the supply phase and the crystal phase determines whether a crystal grows, dissipates or is in equilibrium with the supply phase. This difference, termed supersaturation ($\triangle\mu$), can explicitly be written as:

$$\triangle\mu_{sc} = \mu_s - \mu_c \tag{1.2}$$

In equation 1.2 μ_s and μ_c denote the chemical potential of the supply phase and the crystal phase respectively. Crystal growth is thermodynamically allowed if the supersaturation $\triangle\mu_{sc}$ is positive, since a driving force then exists for adding material to the crystal phase. A continuous supply of material to the supply phase ensures continued crystal growth as material incorporates into the crystal, i.e., a steady-state condition is achieved. If no more material is supplied the supersaturation would decrease, and the supply and crystal phase will at some point reach equilibrium where no chemical potential difference exists between them, i.e., $\triangle\mu_{sc} = 0$.

Even though thermodynamics govern the possibility of crystal growth kinetic factors also play a crucial role in determining the final quality and structure of the crystal. Kinetic factors control the rate at which processes occur and a good example of a kinetic factor is the diffusion of growth material on a crystal surface.

An atomistic model of crystal growth provides a complementary insight for understanding the growth process. In this model the adatoms are viewed as building blocks that incorporate into the crystal. In the growth process, the adatoms are first supplied to the crystal surface by a supersaturated supply phase. The adatoms can then diffuse on the crystal surface and either incorporate into the crystal or desorb back into the supply phase. In order for an adatom to be incorporated it has to form a sufficient number of bonds to keep it from desorbing. Some sites on the crystal surface will be more favorable for incorporation than others. Incorporation preferentially occurs at atomic steps or kinks where the possibility of several bonds exists. On an atomically smooth surface incorporation can also take place once a nucleus has formed. A nucleus can form if a sufficient number of adatoms bond to make it stable.[1]

2 Overview of Growth and Characterization Techniques

The following chapter intends to give a brief overview of the different experimental techniques that have been used in this thesis. This includes descriptions of the nanowire growth setup as well as electron microscopy and optical techniques used to determine material quality and properties.

2.1 Nanowire Growth Setup

Three main ingredients are required in order to form nanowires:

1. The material constituents that build up the nanowire material.
2. An asymmetry that promotes the material constituents to form in a one-dimensional manor.
3. Energy to allow for atomic rearrangements into the desired structure.

The material constituents can be provided either as atomic species (in the form of single atoms or molecules containing a single atomic element), which is used in physical growth techniques such as molecular beam epitaxy (MBE) and laser ablation, or as precursors, which is used in the present growth technique as well as in metal-organic vapor phase epitaxy (MOVPE), chemical beam epitaxy and solution based nanowire growth. Precursors are molecules where the material intended to be incorporated into the nanowire is chemically bonded to one or more

different atomic species that are not intended to be incorporated into the nanowire.

An asymmetry to form nanowires can for example be provided by using a seed particle[2, 3] or an inert mask template[4]. When forming crystalline nanowires one or both of these asymmetries will together with differences in surface energy for different crystal faces give the final one-dimensional structure.

Energy that allows for atomic rearrangements, as well as enhancing chemical reactions, is usually provided in the form of heat. Heat can be provided to only part of the growth system, for example a substrate, using a cold wall reactor or to the entire growth system using a hot wall reactor.

In the following sections details about the aerotaxy growth setup will be given. The numbers that are given, for example flows and temperatures, are specific for the growth experiments carried out in Paper I and later presented in detail in chapter 3. All of these parameters can of course be adapted to suit the experiment you want to perform and the results you wish to achieve.

2.1.1 Aerosol Seed Particle Generation

An aerosol is a gas which contains suspended liquid or solid particles. The term includes both the gas and the particles but can also be used to only describe the particles, neglecting the surrounding gas. For nanowire growth Au is the most widely used and versatile seed particle[5]. In order to generate an aerosol consisting of Au particles an evaporation/condensation method can be used. A piece of Au is in this case heated to between 1,750 and 1,850 °C and a flow of N_2 carrier gas transports the generated Au vapor away from the hot zone. Upon cooling the Au vapor condensates to form primary particles which later agglomerates into agglomerate particles.

After agglomerate formation the particles are charged to allow for size filtering with a differential mobility analyzer (DMA). The DMA filters

the particles according to their electrical mobility which depends on their diameter and electrical charge, and the output particle diameter can be tuned by varying the electric field inside the DMA. The diameter of an agglomerate particle will depend on the particle shape and can thus be the same even though the volume of Au is different, limiting how narrow width distribution it is possible to achieve. In order to improve this a setup with two DMAs can be used instead[6].

After size filtering the agglomerate particles are compacted, into spherical particles, by passing through a sintering furnace set at a temperature of 450 °C. A schematic summarizing the particle formation and size filtering process can be seen in figure 2.1. This method has been used to generate Au particles in the size range of 5-80 nm.

2.1.2 Aerotaxy Growth Reactor

A N_2 carrier gas flow carries the particles and nanowires through the growth system which operates at atmospheric pressure. Material for the nanowire growth is supplied in the form of metal-organic molecules and hydrides. The delivery system is schematically outlined together with the particle formation system in figure 2.1. For growth of GaAs nanowires the precursor of choice for the group III atom is trimethylgallium (TMGa) which consists of one Ga atom attached to three methyl groups. The TMGa is supplied through a standard metal-organic bubbler which is held at a controlled temperature. By passing a carrier gas flow of H_2 through the bubbler some of the TMGa vapor is extracted. The amount of carrier gas is controlled through a mass flow controller (MFC). By changing the carrier gas flow or bubbler temperature the amount of extracted TMGa can be varied. The group V atom is in the case of GaAs supplied in the form of arsine which consists of one arsenic atom and three hydrogen atoms. Arsine has a high vapor pressure and can thus be supplied directly through a MFC without using a carrier gas flow.

The precursor flows are mixed with the aerosol flow before entering the growth reactor. The growth reactor itself consists of a sintered Al_2O_3

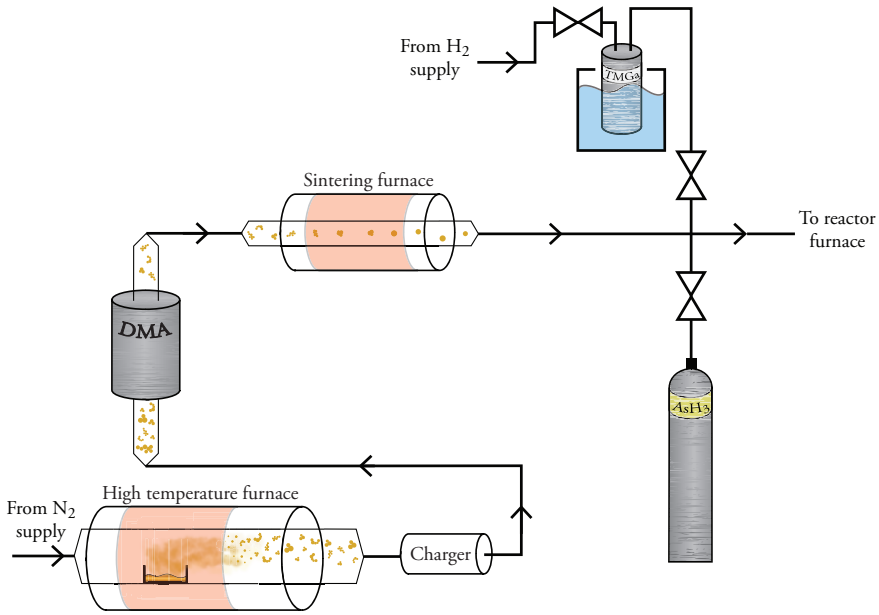

Figure 2.1: Schematic outlining the Au particle formation and gas injection system of the Aerotaxy growth setup. Au particles are generated by an evaporation/condensation method before they are size filtered and compacted. The compacted spherical particles travels in a N_2 carrier gas to which TMGa and AsH_3 is added before it enters the growth reactor.

tube surrounded by a resistive heater and is thus a hot wall reactor. The Al_2O_3 tube is replaceable and different tube diameters can be used in order to change the gas speed inside the reactor.

The flow pattern inside a reactor is important in order to predict and interpret experimental results. A turbulent flow would for example result in an unknown spread in residence time of the particles / nanowires. In contrast to this a laminar flow offers a predictable flow pattern which can be analyzed. An insight whether the flow inside the reactor is laminar or turbulent is given by the Reynolds number:

$$Re = \frac{D\bar{v}\rho_m}{\eta} \tag{2.1}$$

In equation 2.1 D is a typical length in the system, $\bar{v}$ is the mean gas velocity, η is the dynamic viscosity and ρ_m is the mass density. For the values given in table 2.1 $Re = 38$, which is typical for a CVD system and well below the laminar to turbulent flow transition which occurs at $Re = 1200$. A laminar flow inside the reactor means that the flow velocity distribution is parabolic with a maximum value in the center of the reactor and zero velocity at the reactor walls due to viscous drag. This in turn means that a distribution in residence time for each Au particle / nanowire can be expected. This results in a built in length distribution of the grown nanowires in this type of reactor setup.

Table 2.1: Values for calculating the Reynolds number of the aerotaxy reactor

D(Reactor diameter)	$3.2 \cdot 10^{-2}$ m
$\bar{v}$	$0.1\,{}^{\mathrm{m}}/_{\mathrm{s}}$
η	$3.7 \cdot 10^{-5}\,{}^{\mathrm{kg}}/_{\mathrm{ms}}$
ρ_m	$0.44\,{}^{\mathrm{kg}}/_{\mathrm{m}^3}$

In order to understand whether the nanowires will interact with each other during nanowire growth the mean free path (l) of a molecule in the vapour can be compared to the distance between two nanowires (L). In a typical epitaxy growth system this comparison is expressed by the Knudsen number (Kn), defined as:

$$Kn = {}^{l}/_{L} \tag{2.2}$$

In this expression L is usually taken as the distance between material source and deposition substrate. If $Kn > 1$ growth takes place in the

molecular regime, typical in for example MBE. For $Kn < 0.01$, which is typical for CVD reactors, growth takes place in the fluid regime where the vapour can be treated as a continuum and processes such as diffusion are important. The mean free path l is calculated through:

$$l = \frac{1}{\sqrt{2}\pi a^2 n} \tag{2.3}$$

where a is the molecule diameter and n is the number of molecules per unit volume. For $a = 0.3\,\mathrm{nm}$ and $n = 2.4 \cdot 10^{25}\,\mathrm{mcs/m^3}$, l becomes $103\,\mathrm{nm}$. L could be taken as the distance between two adjacent seed particles in the gas and since the aerosol contains $1 \cdot 10^{12}\,\mathrm{particles/m^3}$, the particle to particle distance is $1 \cdot 10^{-4}\,\mathrm{m}$. This gives $Kn = 1 \cdot 10^{-3}$ which is in the fluid regime. This means that synergetic effects, which have been observed in certain substrate based nanowire growth systems[7], is not to be expected unless the total pressure is reduced or the number of seed particles is increased. Except for synergetic effects the distance between adjacent seed particles is important with respect to precursor utilization. If the mean distance between each seed particle is optimized with respect to the volume from which each nanowire collects growth material, precursor utilization can be maximized. This is a major difference compared to a MOVPE process where only precursors traveling close to the substrate surface can decompose and incorporate into the crystal. Taking this into consideration one can expect higher precursor utilization in the aerotaxy process compared to MOVPE.

The actual nanowire production capacity of the aerotaxy reactor in the configuration presented above is about $1.0 \cdot 10^{11}$ nanowires/h . Comparing this to a research MOVPE tool, which has a 2" capacity and the Au particles have been deposited at a density of $1\,\mu\mathrm{m}^{-2}$, the aerotaxy reactor can produce 50 times more nanowires per unit time [Paper I].

2.1.3 The Complete Aerotaxy Growth System

The entire aerotaxy growth system is outlined in figure 2.2. The different parts of the system are connected through stainless steal pipes

and vacuum connections. After the growth reactor the aerosol can be directed to either an electrometer which counts the amount of charge in the aerosol or to a deposition chamber. The deposition chamber contains a collector plate, where a substrate can be placed, connected to a high voltage source. Once the voltage is turned on the charged nanowires are deposited on the substrate.

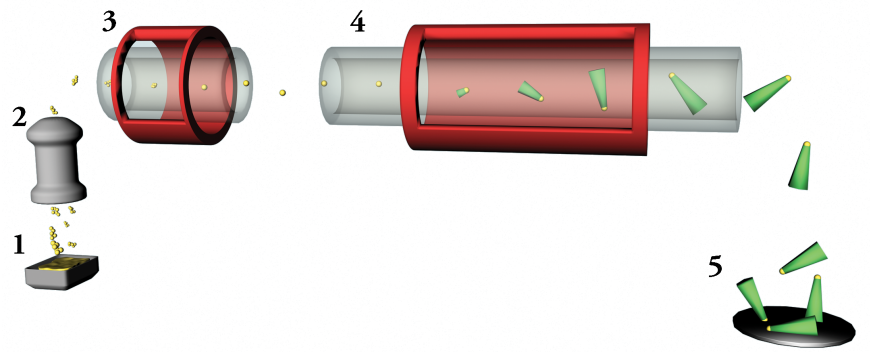

Figure 2.2: Overview of the complete Aerotaxy growth system with (1) Au agglomerate formation, (2) Au agglomerate size filtering, (3) Au agglomerate compaction to spherical particles in a sintering furnace, (4) nanowire growth after adding precursors to the aerosol and (5) nanowire deposition on a substrate.

2.2 Electron Microscopy

The study of nanoscale objects require instruments with resolution beyond that of optical instruments such as the visible light microscope. The image resolution of a light microscope is ultimately limited to approximately half the wavelength of the light used to form the image. In

this case resolution describes the ability to separate two points through a variation in image contrast. It can be noted however that visible light can be used to study and determine object properties well beyond the resolution of a light microscope by using for example Ellipsometry[8] or spectroscopic techniques[9]. In those cases however no directly interpretable image is formed and modeling must be used to extract the object properties.

The electrons used in electron microscopes have a much shorter wavelength compared to visible light. The electron wavelength is determined by the acceleration voltage of the microscope and can vary from approximately 0.01 nm in a scanning electron microscope (SEM) to 0.002 nm in a transmission electron microscope (TEM). Since inter-atomic distances are on the order of 0.2 nm in materials considered here, this appears to be more than enough in order to resolve even the finest details. Limitations in the image forming system will however impose restrictions on how high resolution that can be achieved.

2.2.1 Transmission Electron Microscopy

In a TEM an electron beam is transmitted through a sample and interactions between the electrons and the sample give rise to several different image forming mechanisms. Besides the formation of an image, a TEM can also provide chemical information if it is equipped with analytical tools, for example X-ray Energy Dispersive Spectrometry (XEDS). Before discussing the image formation in a TEM a brief description of the actual instrument is given below.

Figure 2.3 shows a typical TEM column with indicated components. The top of the column consists of an electron gun, in this case a Field Emission Gun (FEG). This type of electron gun extracts electrons by applying an intense electric field over a fine tip of ZrO_2 coated W. The emitted electrons are then accelerated by a set high voltage, 300 kV in the microscope used. Once the electrons are accelerated they reach the first set of electromagnetic lenses, called condenser lenses. These lenses shape the electron beam either as a parallel beam, used in TEM

mode, or as a fine probe, used in Scanning-TEM (STEM) mode. In TEM mode the image is formed by the objective lens after the parallel electron beam has gone through the specimen. Imperfections in the objective lens, such as spherical aberration, set the limit for how high resolution the microscope is capable of. The last major set of lenses are the intermediate and projector lenses, which magnify the formed image from the objective lens and projects it onto the viewing equipment, such as a fluorescent screen or a CCD camera.

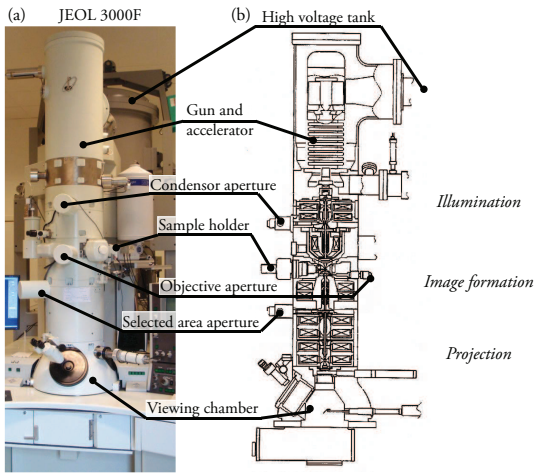

Figure 2.3: (a) Photo of the 300kV JEOL 3000F TEM in Lund (Image courtesy of G. Karlsson). (b) Schematic of the TEM column with some indicated components (courtesy of M. Ek).

Image formation in TEM depends on the interaction between the electrons traveling down the column and the specimen. The electrons can be considered as waves that have a certain amplitude and phase. In low resolution imaging, i.e., images without atomic resolution, amplitude contrast dominates. Amplitude contrast can be divided into mass-thickness contrast and diffraction contrast. Mass-thickness contrast originates, as the name implies, from a variation in mass and/or thickness of the sample. Depending on the atomic number (mass) and the

number of atoms an electron will interact with (thickness) the probability of the electron undergoing a scattering event will change. More mass or more thickness will increase the amount off scattering and thus produce darker areas in a bright-field image. Mass thickness contrast is most important in amorphous and biological samples. Diffraction contrast appears for crystalline samples. A crystalline sample will diffract the electrons at certain angles, in accordance with Bragg's law, and form a diffraction pattern consisting of multiple beams or spots. By orienting the sample in such a way that only two of the beams are excited, for example the direct 000 beam and the 111 beam, the area of the sample where the Bragg condition is fulfilled will appear bright. This can be used to obtain orientation specific information about the sample.

Phase contrast imaging is used in order to obtain images with atomic resolution. In this case multiple diffracted beams are usually used which imposes restrictions on how the sample is oriented with regards to the incoming electron beam. The sample must be oriented along a zone-axis in order to fulfill the Bragg condition for several planes in the crystal. Once the electrons enter the sample they interact with the potential created by the atoms inside it which induces a phase shift of the electron wave. An additional phase shift is then added by the microscope itself where the main contributors, for a well aligned microscope, is spherical aberration and defocus. If the phase shift between a diffracted and non-diffracted electron is π they can interfere destructively and thus give rise to a dark area in the formed image. This dark area would then correspond to the volume of atoms in the sample which gave rise to the original phase shift.

2.3 Photoluminescence

In photoluminescence (PL) a sample is excited with light, usually from a laser with a fixed wavelength above the bandgap of the studied material, which creates electron-hole pairs also known as excitons. The

electrons and holes will, after excitation, recombine at a rate determined by the lifetime and amount of excess minority carriers. Before recombination they can thermalize in order to reach lower energy states and if most states are unoccupied they will thermalize to the band edge (see figure 2.4). The recombination can either be radiative, which can give information about the bandgap (E_g) or states lying close to the bandgap, or non-radiative, which can occur through a series of mid-gap defect or surface states. The PL peak position(s) and full width at half maximum (FWHM) can give information on the purity of the studied material or what type of defects that are present.

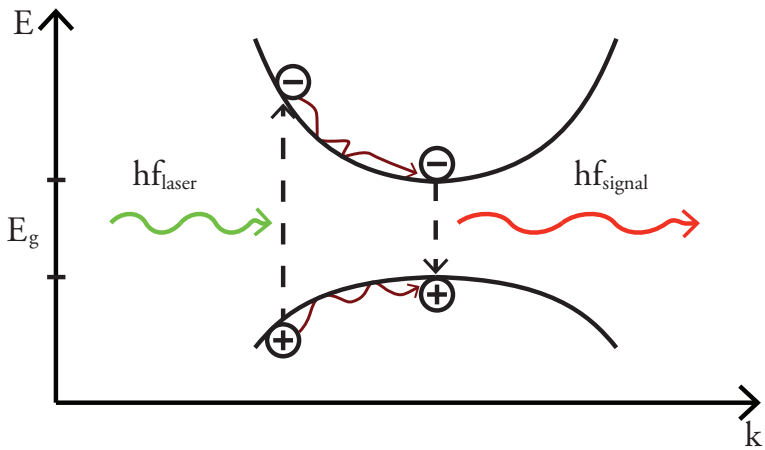

Figure 2.4: Schematic of the excitation and recombination processes during a PL experiment. In this case light from a green laser (hf_{laser}) excites an electron-hole pair in the material which then thermalize and recombine close to the band edge, emitting light of a longer wavelength (hf_{signal}). We can note that the relation between the photon energies follows $hf_{laser} > hf_{signal}$.

3 Nanowire growth in an Aerosol

The following chapter starts with an introduction to particle assisted nanowire growth based on the available knowledge from mainly substrate based approaches. After this a detailed description and discussion on the results obtained when growing nanowires with the Aerotaxy technique is presented.

3.1 Particle Assisted Nanowire Growth

Particle assisted wire growth was first investigated in the 1960's, by using Au particles to form elongated Si crystals[10]. This early work proposed a model for the growth behavior, termed Vapor-Liquid-Solid (VLS), in which it is described that the seed particle, which is in a liquid state, acts as a sink or catalyst for the growth species and is thus able to promote one-directional growth. Although this model tried to explain growth of wires measuring 100's of µm's up to mm's in diameter many of the concepts has been transferred into the nano-regime. VLS can however not explain all instances of nanowire growth that have been observed and some key issues that can not be explained are:

1. The particle should act as a sink which implies that it is at a lower chemical potential (μ_{particle}) than the supply phase (μ_{vapor}). However, in order for the one directional growth to take place μ_{particle} has to be larger than μ_{solid} since there should be a driving force to precipitate material underneath the particle. This gives the relation $\mu_{\text{vapor}} > \mu_{\text{particle}} > \mu_{\text{solid}}$ which implies the the supersaturation and thus driving force for growth is largest between

the vapor and solid and not at the interface between particle and solid.

2. Nanowire growth has been observed also in physical deposition techniques, such as MBE[11], where no catalyst should be required to enhance chemical reactions.

3. The state of the particle has been observed to not always be liquid[12, 13].

To overcome these issues it has been proposed that it is the nucleation that is enhanced by the particle[14]. In this model the particle (which can be liquid or solid) acts as a collector of material and there is an enhanced nucleation rate at the boundary between the particle, vapor and solid. Formation of a nucleus is equivalent to adding a new atomic layer with a limited size at the particle-solid interface. The step that is formed between the nucleus and the previous layer can then propagate under the entire particle-solid interface by so called step-flow growth, before the process repeats itself.

Recently further refinements of nanowire growth theory have been made after experimental findings from in-situ TEM[15, 16, 17]. By observing nanowire growth in real time a truncated facet at the vapor-particle-solid interface has been found and nucleation should thus be considered to take place as an extension of this truncated facet. Nucleation would then occur at the particle-solid interface instead of the vapor-particle-solid boundary. In addition to this an oscillating behavior of the facet, directly related to the supersaturation in the droplet, indicates that growth occurs in a step-flow process.

3.2 Aerotaxy

Most investigations of semiconductor nanowires have been performed using a substrate as a base for the grown material. Substrate based nanowire growth thus provides the foundation for understanding the nanowire growth mechanism explored in the previous section. Although

gas phase growth of nanocrystals in general and nanowires in particular have been less frequently reported in literature, several key technological achievements have been made. Early work by Lieber et. al. showed an impressive generality for the growth of different semiconductor materials in the gas phase from metal particles[18]. In this report laser ablation, also termed Laser Catalytic Growth, of metal coated semiconductor targets is used to produce nanowires with lengths exceeding 10's of µm's and diameters varying from 3 to 30 nm. In this way nanowires of the materials GaAs, GaP, InAs, InP, as well as InAsP and GaAsP alloys along with several II-VI materials, and different SiGe alloys could be fabricated.

The main drawbacks of previous nanowire gas phase growth techniques has been the lack of control of nanowire diameter, length and shape and the need for a substrate to provide the growth material. The nanowire diameter is a critical parameter since it affects the electronic[19] and optical[20] properties of the material. Previous studies of gas phase fabrication of semiconductor nanocrystals[21] and carbon nanotubes[22] have shown that an aerosol based approach can both tune and narrow the diameter range of the produced nanostructure.

3.2.1 Nucleation

Nucleation is one of the key issues when investigating gas phase nanowire growth. It is however difficult to study separately since it is an inherent part of the nanowire growth itself. As long as the same reactor furnace is used for the nucleation and growth of the nanowires, studies of the nucleation can only come from ex-situ TEM investigations. It is possible that parameters such as growth temperature and precursor flows for optimal nucleation and nanowire growth are not the same, but due to the nature of the process they are inevitably related.

Figure 3.1 shows three examples of TEM investigations of the nanowire base. The base can vary from containing very few defects (figure 3.1a), i.e., only a few stacking faults inclined from the growth direction, to being partially poly-crystalline (figure 3.1b,c). Typically the nanowire

base is most crystalline at low growth temperatures (<525 °C). At higher temperatures the poly crystalline base is typically larger. This could have several causes, for example a different size of the seed particle (which becomes supersaturated with Ga) or increased amount of parasitic vapor-solid growth due to a lower kinetic barrier.

The nucleation process itself most likely starts by the supersaturation of Ga in the Au particle. Some of this material is then precipitated on the Au particle surface where it crystallizes in the presence of As. Since there is no substrate or seed crystal to guide the crystallization the most likely result is formation of a poly-crystalline material. At some point there is however the chance that a <111> plane is generated and once this forms the nanowire growth can proceed by formation of subsequent <111> planes extending the nanowire in the <111> direction.

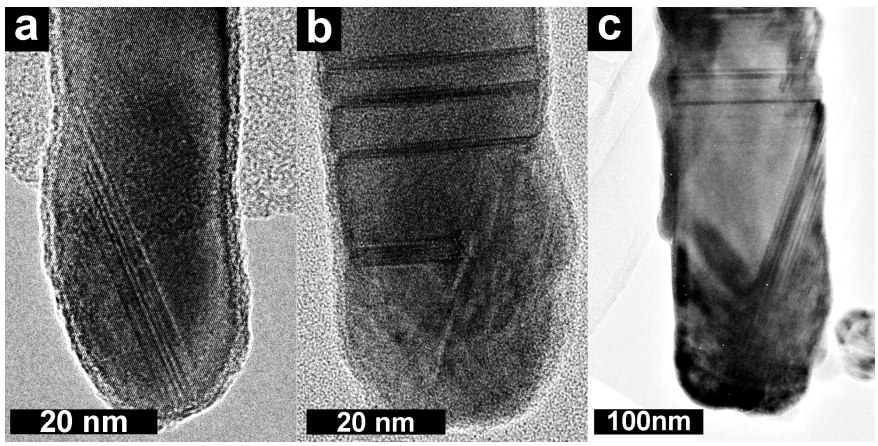

Figure 3.1: Three examples of TEM images showing the nanowire base and how the crystallinity at the point of nucleation can vary. (a) and (b) were nucleated at a temperature of 450 °C and (c) at a temperature of 575 °C.

3.2.2 Control of nanowire dimensions

By using the growth setup outlined in section 2.1 it is possible to control the nanowire diameter (figure 3.2). The diameter is set by the Au particle size which is determined by the DMA which filters Au agglomerates of a certain size according to its applied voltage. The standard deviation of the top diameter of the grown nanowires is between 5-10 nm but could be improved by for example adding a second DMA as discussed in section 2.1.1.

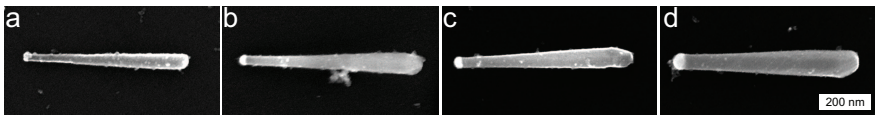

Figure 3.2: Scanning electron microscope images of Aerotaxy grown GaAs nanowires. (a-d) shows nanowires grown with 35- (a), 50- (b), 70- (c) and 120-nm (d) diameter Au agglomerates which result in average nanowire top diameters of 30, 41, 51 and 66 nm, respectively.

Besides the diameter at the top, which is set by the Au particle, an additional diameter variation along the nanowire length, known as tapering, is caused by vapor-solid growth. This is material that is grown on the nanowire side facets directly from the vapor, especially at higher temperatures (see figure 3.3), and is a known issue also for substrate based growth techniques. This effect can be reduced by tuning the growth parameters or introducing a suitable etchant[23].

The nanowire growth rate increases exponentially with temperature [Paper I] but saturates after 550 °C (see figure 3.3e). Interestingly the growth rate does not decrease after this, which is reported for substrate based nanowire growth[24], but maintains an almost constant value. The difference originates in the use of a substrate on which parasitic growth can take place. Similarly, parasitic growth can also occur in the gas phase, forming particles, but since the particle-particle distance is quite large (see section 2.1.2) this does not influence the growth rate significantly at the investigated temperatures.

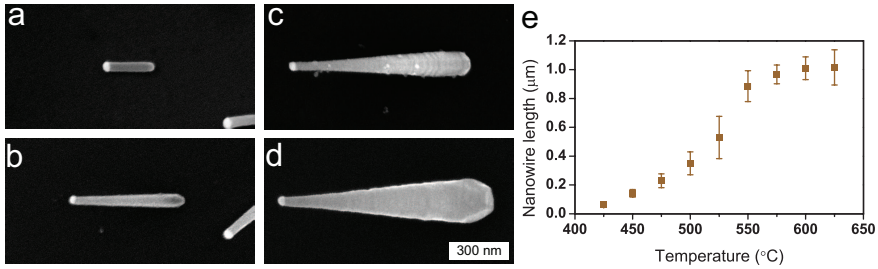

Figure 3.3: Nanowires grown with 50 nm Au agglomerates at different temperatures showing different amount of tapering and thus shape. The furnace temperature was set at 450 (a), 500 (b), 550 (c) and 600 °C (d). (e) shows the nanowire length dependance on the growth temperature.

In order to change the nanowire growth time the gas speed inside the reactor should be different (for a given furnace length). It is possible to change the gas speed either by changing the reactor tube diameter, changing the total gas flow or changing the pressure. From these options changing the reactor tube diameter has the smallest effect on overall growth conditions (besides that it changes the growth time). We have tried two different tube diameters, 18 and 32 mm, which give approximate average growth times of 0.3 and 1 s (see figure 3.4). As the nanowires spend longer time in the hot zone of the furnace more time is available for them to elongate, as long as the precursors are not depleted during growth.

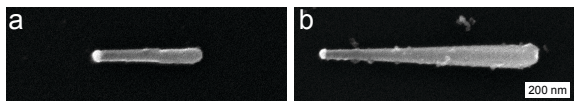

Figure 3.4: Scanning electron microscope images of nanowires grown with two different reactor tubes resulting in a growth time of approximately 0.3 (a) and 1 s (b).

3.2.3 Crystal structure

TEM images of nanowires grown at different temperatures is shown in figure 3.5. At low growth temperatures (T < 525 °C) the grown nanowires have a pure zinc-blende crystal structure without stacking defects. As the temperature is increased beyond this the number of stacking defects increase, which follows the same trend observed in substrate nucleated VLS nanowires[25]. Detailed studies of the nanowire growth direction also show that it coincides with the most prominent growth direction of substrate based nanowires, <111>B [Paper I].

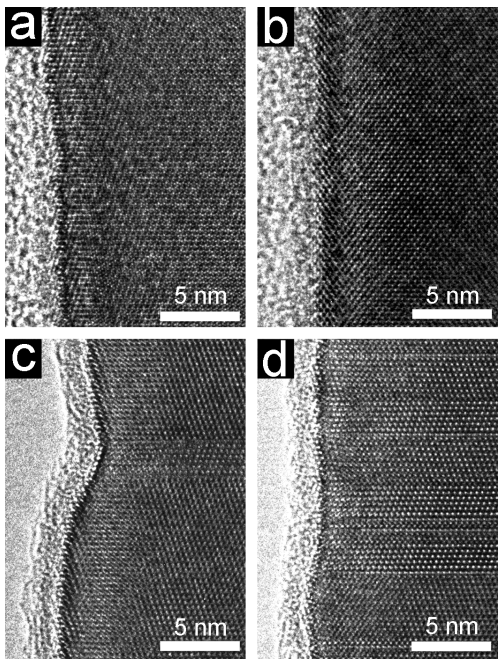

Figure 3.5: TEM images of nanowires grown at 450 (a), 500 (b), 550 (c) and 600 °C. As temperature increases the number of stacking defects (in this case twin planes) also increases.

3.2.4 Optical properties

The optical properties of a set of these nanowires has been investigated using a PL setup (figure 3.6). The nanowires were grown at a relatively high growth temperature (625 °C) in order to suppress carbon incorporation from the TMGa molecule. PL of nanowires grown at lower temperatures often show luminescence below the bandgap of GaAs which can be attributed to a reduction in bandgap caused by non-intentional p-type doping of carbon. The PL contains a main peak at 1.514 eV which corresponds to the known range of free and bound excitons in GaAs (1.513-1.516 eV [26]). The average full width at half maximum of 8 different measurements was 23 meV [Paper I] which is comparable or better than GaAs nanowires grown on a Si substrate[27].

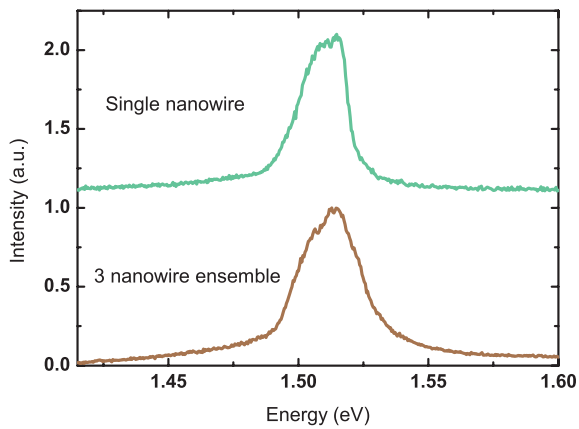

Figure 3.6: Micro-PL measurements obtained from a single nanowire and a 3 nanowire ensemble. The main peak is located at 1.514 eV and the FWHM of 8 different nanowire ensembles is 23 meV. (a.u. arbitrary units)

4 Conclusions and Outlook

The results obtained in this thesis show that it is possible to efficiently fabricate semiconductor nanowires of high quality using a gas phase technique. Most importantly we showed that control of nanowire size, shape and crystal structure is possible. The optical properties of nanowires grown in the gas-phase is comparable to those obtained from nanowires grown on a substrate, which is important for future integration of gas-phase nanowires in opto-electronic devices.

Currently there is a large effort on continued development both from a material science and device integration perspective. Design of an improved rector setup is crucial in order to reduce nanowire variations and increase material yield. Extending the concept to more materials besides GaAs as well as combining different materials in the same nanowire by for example using sequential furnaces will be important future goals. Device integration is certainly challenging since any opto-electronic device would need alignment of the nanowires in order to facilitate contact formation. This certainly ensures that research on gas-phase nanowire growth and its applications will continue for many years to come with hopefully new and exciting results.

Bibliography

[1] Burton, W. K., Cabrera, N. & Frank, F. C. The growth of crystals and the equilibrium structure of their surfaces. *Philosophical Transactions of the Royal Society of London. Series A, Mathematical and Physical Sciences* **243**, 299–358 (1951).

[2] Yazawa, M., Koguchi, M., Muto, A., Ozawa, M. & Hiruma, K. Effect of one monolayer of surface gold atoms on the epitaxial growth of InAs nanowhiskers. *Applied Physics Letters* **61**, 2051–2053 (1992).

[3] Morales, A. M. & Lieber, C. M. A laser ablation method for the synthesis of crystalline semiconductor nanowires. *Science* **279**, 208–211 (1998).

[4] Motohisa, J., Noborisaka, J., Takeda, J., Inari, M. & Fukui, T. Catalyst-free selective-area MOVPE of semiconductor nanowires on (111)B oriented substrates. *Journal of Crystal Growth* **272**, 180 – 185 (2004).

[5] Messing, M., Hillerich, K., Johansson, J., Deppert, K. & Dick, K. The use of gold for fabrication of nanowire structures. *Gold Bulletin* **42**, 172–181 (2009).

[6] Magnusson, M. H., Deppert, K., Malm, J.-O., Bovin, J.-O. & Samuelson, L. Size-selected gold nanoparticles by aerosol technology. *Nanostructured Materials* **12**, 45–48 (1999).

[7] Borgström, M. T., Immink, G., Ketelaars, B., Algra, R. & Bakkers, E. P. A. M. Synergetic nanowire growth. *Nature Nanotechnology* **2**, 541–544 (2007).

[8] Fujiwara, H., Kondo, M. & Matsuda, A. Real-time spectroscopic ellipsometry studies of the nucleation and grain growth processes in microcrystalline silicon thin films. *Physical Review B* **63**, 115306 (2001).

[9] Anttu, N. *et al.* Optical far-field method with subwavelength accuracy for the determination of nanostructure dimensions in large-area samples. *Nano Letters* **13**, 2662–2667 (2013).

[10] Wagner, R. S. & Ellis, W. C. Vapor-liquid-solid mechanism of single crystal growth. *Applied Physics Letters* **4**, 89–90 (1964).

[11] Dheeraj, D. L. *et al.* Growth and characterization of wurtzite GaAs nanowires with defect-free zinc blende GaAsSb inserts. *Nano Letters* **8**, 4459–4463 (2008).

[12] Persson, A. I. *et al.* Solid-phase diffusion mechanism for GaAs nanowire growth. *Nature Materials* **3**, 677–681 (2004).

[13] Dick, K. A. *et al.* Failure of the vapor-liquid-solid mechanism in Au-assisted MOVPE growth of InAs nanowires. *Nano Letters* **5**, 761–764 (2005).

[14] Wacaser, B. A. *et al.* Preferential interface nucleation: An expansion of the VLS growth mechanism for nanowires. *Advanced Materials* **21**, 153–165 (2009).

[15] Oh, S. H. *et al.* Oscillatory mass transport in vapor-liquid-solid growth of sapphire nanowires. *Science* **330**, 489–493 (2010).

[16] Gamalski, A. D., Ducati, C. & Hofmann, S. Cyclic supersaturation and triple phase boundary dynamics in germanium nanowire growth. *The Journal of Physical Chemistry C* **115**, 4413–4417 (2011).

[17] Wen, C.-Y. *et al.* Periodically changing morphology of the growth interface in Si, Ge, and GaP nanowires. *Physical Review Letters* **107**, 025503 (2011).

[18] Duan, X. & Lieber, C. M. General synthesis of compound semiconductor nanowires. *Advanced Materials* **12**, 298–302 (2000).

[19] Ford, A. C. *et al.* Diameter-dependent electron mobility of InAs nanowires. *Nano Letters* **9**, 360–365 (2008).

[20] Anttu, N. & Xu, H. Q. Efficient light management in vertical nanowire arrays for photovoltaics. *Optics Express* **21**, A558–A575 (2013).

[21] Deppert, K. & Samuelson, L. Self-limiting transformation of monodisperse Ga droplets into GaAs nanocrystals. *Applied Physics Letters* **68**, 1409–1411 (1996).

[22] Kim, S. H. & Zachariah, M. R. Gas-phase growth of diameter-controlled carbon nanotubes. *Materials Letters* **61**, 2079–2083 (2007).

[23] Borgström, M. *et al.* In situ etching for total control over axial and radial nanowire growth. *Nano Research* **3**, 264–270 (2010).

[24] Borgström, M., Deppert, K., Samuelson, L. & Seifert, W. Size- and shape-controlled GaAs nano-whiskers grown by MOVPE: a growth study. *Journal of Crystal Growth* **260**, 18–22 (2004).

[25] Joyce, H. J. *et al.* Twin-free uniform epitaxial GaAs nanowires grown by a two-temperature process. *Nano Letters* **7**, 921–926 (2007).

[26] Bogardus, E. H. & Bebb, H. B. Bound-exciton, free-exciton, band-acceptor, donor-acceptor, and auger recombination in GaAs. *Physical Review* **176**, 993–1002 (1968). PR.

[27] Moewe, M., Chuang, L. C., Crankshaw, S., Chase, C. & Chang-Hasnain, C. Atomically sharp catalyst-free wurtzite GaAs/AlGaAs nanoneedles grown on silicon. *Applied Physics Letters* **93**, 023116–3 (2008).